Large area confocal microscopy

D. Yelin, C. Boudoux, B. E. Bouma, and G. J. Tearney

Wellman Center for Photomedicine, Massachusetts General Hospital, 55 Fruit Street, BAR 703, Boston, Massachusetts 02114, USA

Received December 8, 2006; revised January 16, 2007; accepted February 1, 2007; posted February 5, 2007 (Doc. ID 77949); published April 3, 2007

Imaging large tissue areas with microscopic resolution *in vivo* may offer an alternative to random excisional biopsy. We present an approach for performing confocal imaging of large tissue surface areas using spectrally encoded confocal microscopy (SECM). We demonstrate a single-optical-fiber SECM apparatus, designed for imaging luminal organs, that is capable of imaging with a transverse resolution of 2.1 μm over a subsurface area of 16 cm^2 in less than 1 min. Due to the unique probe configuration and scanning geometery, the speed and resolution of this new imaging technology are sufficient for comprehensively imaging large tissues areas at a microscopic scale in times that are appropriate for clinical use. © 2007 Optical Society of America

OCIS codes: 110.0180, 170.2150, 170.1790.

Random excisional biopsy is conducted when dysplasia or cancer is suspected, but not visible by conventional radiologic techniques or by gross inspection. Sampling errors leading to missed diagnoses are common with random biopsy, since the disease may be present focally within a large tissue area and the biopsy forceps only sample a small fraction of the tissue under investigation. A technology for comprehensively obtaining microscopic diagnoses from large epithelial surfaces within patients could be used to guide the biopsy procedure, thereby providing diagnoses that are more representative of the true disease state.

Reflectance confocal microscopy[1] (RCM) is particularly well suited for noninvasive diagnosis in patients as it is capable of measuring microscopic structure without tissue contact and does not require the administration of extrinsic contrast agents. RCM rejects out of focus light and detects backscattered photons only from a single plane within the tissue. While RCM has been extensively demonstrated in the skin,[2,3] development of endoscopic confocal microscopy systems has taken longer due to the substantial technical challenges involved in miniaturizing a scanning microscope. A variety of approaches for addressing this problem[4–13] include the use of microelectromechanical systems (MEMS) scanning mirrors[4] and single-mode fiber bundles.[5–8] Solutions for the miniaturization of high NA objectives include a gradient-index lens system,[9] dual-axis objectives,[10] custom designs of miniature objectives,[11] and micro-objectives.[6]

Even though endoscopic reflectance[12] and fluorescence[8,13] confocal microscopy have been demonstrated in patients, these techniques have not yet had a major impact on clinical management. One important reason is that confocal microscopy provides images only at discrete locations—the so-called "point sampling" approach. As currently implemented, point sampling is inherent to confocal microscopy since it has an extremely limited field of view, comparable to or less than that of an excisional biopsy. Some groups have attempted to overcome the limited field by creating image mosaics composed of multiple confocal images.[8] Comprehensive imaging of 5–50 cm^2 internal organ tissue surface areas required for many important screening applications is challenging, however. Frame rates must be significantly increased to reduce artifacts due to sample motion and so that imaging can be accomplished in an acceptable procedure time (~5 min). Tissue surface stabilization and special scanning geometries are needed to cover the entire surface area without gaps.

Spectrally encoded confocal microscopy[14] (SECM) is an alternative approach for *in vivo* reflectance confocal microscopy that is capable of high-speed imaging within an endoscopic probe.[15,16] SECM uses broad bandwidth light and encodes one dimension of spatial information on the sample in the optical spectrum.[14] Since the spectral decoding can be performed rapidly outside the body by means of a fast spectrometer or by using a rapid wavelength swept source,[17] a fast scanning mechanism such as galvanometric scanner, piezoelectric crystals, or rotating polygons scanners is not needed within the probe. Both the broadband-spectrometer and the swept-source approaches are generally comparable in their scanning speeds, but differ mainly in their power and wavelengths. SECM was previously demonstrated with a 440 μm × 400 μm field of view and 1.4 μm resolution.[17] Spectrally encoded endoscopes can be as small as 350 μm in diameter[16] or hand held,[15] while still maintaining video-rate imaging.[16,17]

In this Letter, we use SECM to perform confocal microscopy of areas that are 3–4 orders of magnitude larger than that of single images obtained by conventional confocal microscopes. The proof-of-principle comprehensive SECM device (Fig. 1) was designed to obtain images from within a cylinder with a length of 2.5 cm and a diameter of 2.0 cm, roughly the dimensions of the distal human esophagus. A fiber-coupled 2.0 mW superluminescent diode, centered at 793 nm, and with a bandwidth of 44 nm illuminated a 50/50 single-mode fiber-optic beam splitter. Light transmitted through one port of the splitter was collimated and transmitted through a two-lens focusing apparatus to a grating–lens pair (aspheric lens: f=4.5 mm, =5.0 mm, NA=0.55; grating: 1780 line pairs/mm, Holographix LLC), producing a 500 μm longitudinal

0146-9592/07/091102-3/$15.00

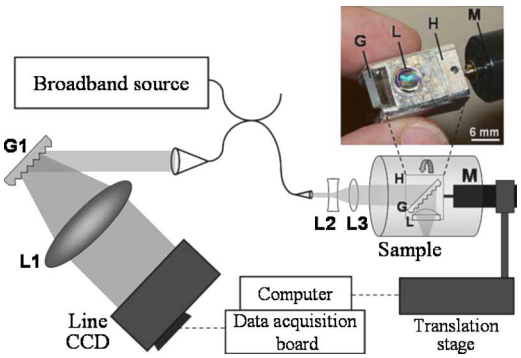

Fig. 1. (Color online) Schematic of the proof-of-principle apparatus for large area confocal microscopy. L, aspheric lens; G, diffraction grating; H, optics housing; M, motor; G1, spectrometer grating; L1, spectrometer lens; L2, L3, focusing lenses.

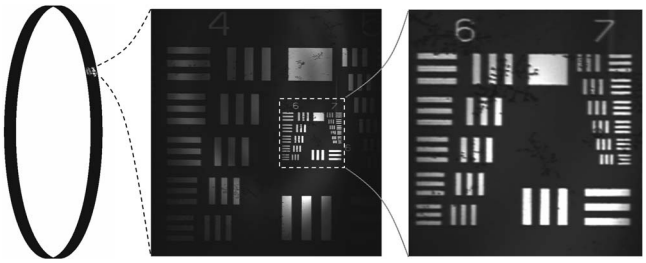

Fig. 2. Image of USAF resolution chart in three magnification steps. The original data set (left) was a 2 cm diameter, 0.5 mm long cylinder.

array of focused, spectrally encoded spots on the interior surface of the cylindrical sample. The grating–lens pair was affixed to a motor (15 mm diameter) shaft by a custom-machined housing. As the motor rotated, the spectrally encoded line was scanned across the sample's inner circumference. Simultaneously, the motor, housing, and lens–grating pair were translated along the longitudinal axis of the cylinder by a computer-controlled linear stage, affecting a helical scan of the entire interior surface of the sample. Light reflected from the sample was transmitted back through the optical system to a custom-built spectrometer and linear CCD (Basler L104K, 30 kHz line rate). To achieve 1.0 μm circumferential sampling, we digitized approximately 60,000 points per motor rotation (30 rpm). The longitudinal velocity of the motor was 0.25 mm/s, and the time required for one complete scan was 100 s.

The $1/e^2$ diameter of the collimated beam on the grating–lens pair was 4.0 mm. As a result, the effective NA of our system was approximately 0.4. The theoretical transverse and axial resolutions of our confocal system was 1 and 3.6 μm, respectively. Assuming an aberration-free system, the theoretical spectral resolution on the sample was 0.08 nm, resulting in a maximum of ~630 resolvable points across the spectrally encoded line. The spectrometer in the detection arm was designed to exceed the spectral resolution of the probe. Figure 2 shows an SECM scan of a 1951 U.S. Air Force resolution chart obtained with this proof-of-principle system. The smallest bars (Group 7, Element 6), which are separated by 2.2 μm, were clearly resolved. The transverse line spread function FWHM and axial FWHM from a mirror scanned through the focus were measured to be 2.1 and 5.5 μm, respectively.

Figure 3 shows SECM image data for a complete pullback image of a 2.5 cm long phantom consisting of lens paper affixed to the inner surface of a 2 cm inner diameter Teflon tube. The focal plane was adjusted by changing the separation between the lenses L2 and L3 (see Fig. 1), allowing imaging at different depths within the sample. Five cylindrical 2D images were acquired at five discrete focal depths over a range of 120 μm, and were summed to create an integrated image (Fig. 3a), demonstrating near-complete coverage of the phantom. In this low mag-

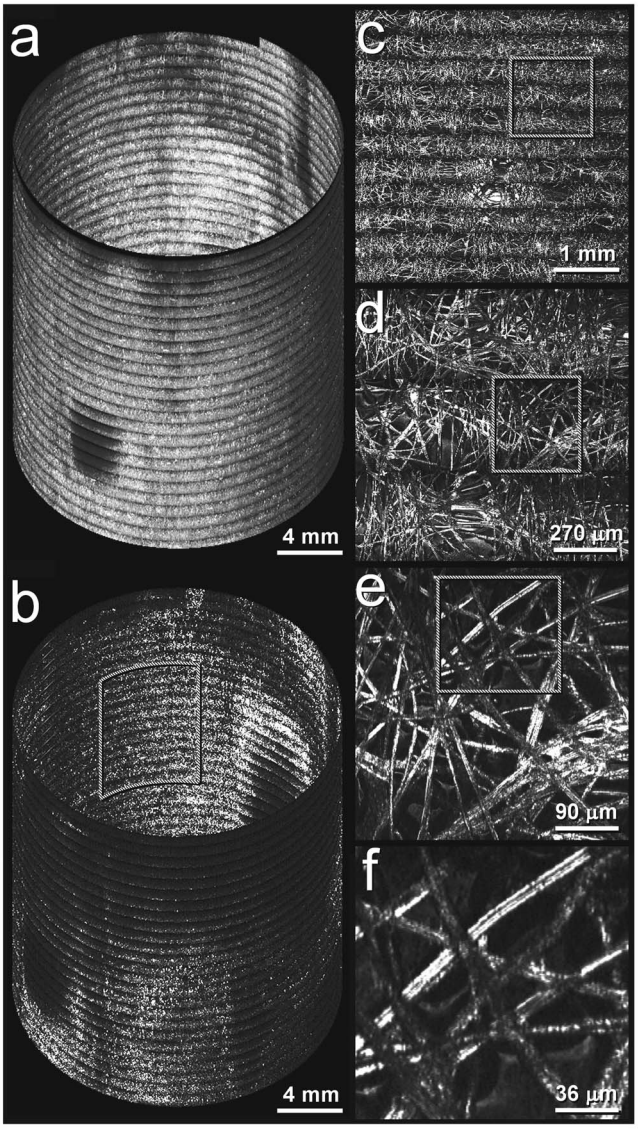

Fig. 3. Comprehensive SECM image data from a lens paper phantom, displayed at increasing magnifications. a, Integrated view of the entire data set. b, Single optical section from the data set in a. c, Magnification of 4.5× of the region of interest marked in b. d, 16.7× magnification of the region marked in c. e, Magnification of 50× of the region marked in d. f, Magnification of 125× of the region marked in e. Rectangles in each image represent the zoomed regions of interest.

nification view (Fig. 3a), the macroscopic structure of the paper, including folds and voids, can be visualized. The data set in Fig. 3a covers an effective area of 78.5 cm^2 and contains 10.5 Gpixels; each 8 bit pixel covers 0.7×1 μm. The total acquisition time was 500 s for all five focal planes. A subset of the full data set, representing a single cylindrical plane within the sample, is shown in Fig. 3b. The diminished spectral intensity at the edges of the spectrum and lens aberrations caused a stripe artifact. When regions of this data set are shown at higher magnifications, individual fibers and fiber microstructure can be clearly resolved (Figs. 3c–3f).

Imaging biological samples with the proof-of-principle apparatus was complicated by the lack of a dynamic centering apparatus for the optical scan head. To provide further support for the principles of wide-field microscopy, however, a sample of swine intestine was placed on a narrow space between two 2.0 cm diameter cylinders, to approximate cylindrical tissue geometry, and a 360° scan was acquired in 1 s (Fig. 4a). Since the probe was not centered and the sample did not form an exact cylindrical shape, tissue appears in only one sector of the cylindrical scan. Magnified images of the tissue are suggestive of glandular structure (Fig. 4b) and demonstrate bright reflective dots that may represent nuclei or intracellular vacuoles (Figs. 4c and 4d). Other areas of the SECM scan show artifacts, including strong reflectance from the tissue surface that saturated the detector, or complete signal dropout (Fig. 4b), both of which resulted from improper positioning of the focused SECM beam.

Challenges remain before this approach can be utilized clinically. Further miniaturization of the optics, motor, and housing are required. Our experimental apparatus shows that for SECM, a single element aspheric lens is capable of sufficient quality imaging and, for many applications, can replace a multielement objective lens[11] that would significantly increase the size of the probe. For internal organ luminal imaging, endoscopes must be designed to ensure precise centering of the imaging optics, so that the focus always remains within the epithelium. In addition, the large amount of data necessitates the development of fast data acquisition and storage systems, as well as software tools for real-time data processing and displaying. Finally, prospective determination of the diagnostic accuracy of SECM for specific clinical applications must be conducted.

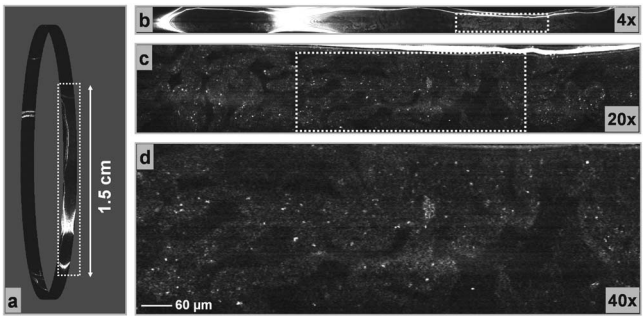

Fig. 4. Circumferential SECM image data from a swine intestinal tissue fragment, displayed at increasing magnifications. With respect to the image depicted in a, the magnifications are as follows: a, 1×; b, 4×; c, 20×; d, 40×. Dotted rectangles in each image represent the zoomed regions of interest.

This study was funded in part by the Center for Integration of Medicine and Innovative Technology and by the National Institutes of Health, National Cancer Institute grant (R21CA122161-01). G. J. Tearney's e-mail address is gtearney@partners.org.

References

1. M. Rajadhyaksha, R. R. Anderson, and R. H. Webb, Appl. Opt. **38**, 2105 (1999).
2. S. Gonzalez, M. Rajadhyaksha, and R. R. Anderson, J. Invest. Dermatol. **111**, 538 (1998).
3. S. Gonzalez, G. Rubinstein, V. Mordovtseva, M. Rajadhyaksha, and R. R. Anderson, J. Cutan. Pathol. **26**, 504 (1999).
4. D. L. Dickensheets and G. S. Kino, Opt. Lett. **21**, 764 (1996).
5. A. F. Gmitro and D. Aziz, Opt. Lett. **18**, 565 (1993).
6. E. Laemmel, M. Genet, G. Le Goualher, A. Perchant, J. F. Le Gargasson, and E. Vicaut, J. Vasc. Res. **41**, 400 (2004).
7. K. Carlson, M. Chidley, K. B. Sung, M. Descour, A. Gillenwater, M. Follen, and R. Richards-Kortum, Appl. Opt. **44**, 1792 (2005).
8. L. Thiberville, S. Moreno-Swirc, T. Vercauteren, E. Peltier, C. Cave, and G. B. Heckly, Am. J. Respir. Crit. Care Med. **175**, 22 (2007).
9. J. Knittel, L. Schnieder, G. Buess, B. Messerschmidt, and T. Possner, Opt. Commun. **188**, 267 (2001).
10. T. D. Wang, M. J. Mandella, C. H. Contag, and G. S. Kino, Opt. Lett. **28**, 414 (2003).
11. C. Liang, K. B. Sung, R. R. Richards-Kortum, and M. R. Descour, Appl. Opt. **41**, 4603 (2002).
12. M. Sakashita, H. Inoue, H. Kashida, J. Tanaka, J. Y. Cho, H. Satodate, E. Hidaka, T. Yoshida, N. Fukami, Y. Tamegai, A. Shiokawa, and S. Kudo, Endoscopy **35**, 1033 (2003).
13. R. Kiesslich, J. Burg, M. Vieth, J. Gnaendiger, M. Enders, P. Delaney, A. Polglase, W. McLaren, D. Janell, S. Thomas, B. Nafe, P. R. Galle, and M. F. Neurath, Gastroenterology **127**, 706 (2004).
14. G. J. Tearney, M. Shishkov, and B. E. Bouma, Opt. Lett. **27**, 412 (2002).
15. C. Pitris, B. E. Bouma, M. Shiskov, and G. J. Tearney, Opt. Express **11**, 120 (2003).
16. D. Yelin, I. Rizvi, W. M. White, J. T. Motz, T. Hasan, B. E. Bouma, and G. J. Tearney, Nature **443**, 765 (2006).
17. C. Boudoux, S. H. Yun, W. Y. Oh, W. M. White, N. Iftimia, M. Shishkov, B. E. Bouma, and G. J. Tearney, Opt. Express **13**, 8214 (2005).